Friction law for atomic-scale contact assisted by atomistic simulations

Yang Wang
Tohoku University
Jingxiang Xu
Shanghai Ocean University
Yusuke Ootani
Institute for Materials Research, Tohoku University
Nobuki Ozawa
Tohoku University
Koshi Adachi
Department of Mechanical Systems Engineering, Graduate School of Engineering, Tohoku University
https://orcid.org/0000-0002-2911-2693
Momoji Kubo (momoji@imr.tohoku.ac.jp)
Tohoku University

Article

Keywords: atomic-scale contact, friction law

Posted Date: February 1st, 2021

DOI: https://doi.org/10.21203/rs.3.rs-149656/v1

Friction law for atomic-scale contact assisted by atomistic simulations

Yang Wang[1, 2], Jingxiang Xu[1, 3], Yusuke Ootani[1], Nobuki Ozawa[1], Koshi Adachi[2], and Momoji Kubo[1, 4] *

[1] Institute for Materials Research, Tohoku University, 2-1-1 Katahira, Aoba-ku, Sendai 980-8577, Japan

[2] Department of Mechanical System Engineering, Graduate School of Engineering, Tohoku University, 6-6-01 Aoba, Aramaki, Aoba-ku, Sendai 980-8579, Japan

[3] College of Engineering Science and Technology, Shanghai Ocean University, 999 Hucheng Ring Road, Pudong, Shanghai 201306, China

[4] New Industry Creation Hatchery Center, Tohoku University, 6-6-10, Aoba, Aramaki, Aoba-ku, Sendai 980-8579, Japan.

*Correspondence to: momoji@imr.tohoku.ac.jp (M. Kubo)

Abstract

Non-empirical law depicting how atomic-scale friction behaves is crucial to facilitate the practical design of tribosystems. However, progress in developing a practically usable friction law has stagnated because atomic-scale friction arises from the continuous forming and rupturing of interfacial chemical bonds and such interfacial chemical reactions are difficult to measure precisely in experiments. Here, we propose a usable friction law for atomic-scale contact by using atomistic simulations to correctly measure the interfacial chemical reactions of a realistic rough surface, and confirm its applicability to predicting how atomic-scale friction varies with temperature, sliding velocity, and load.

Friction is particularly important for reducing energy consumption because around 30% of the world's energy is lost to friction[1,2]. Generally, friction between two solids sliding relative to each other depends on not only the types of contacting materials but also external conditions such as temperature, applied load, and sliding velocity. Practically applicable friction laws that predict how these external conditions influence the friction force are crucial because they would benefit greatly the practical design of lubricating systems.

Conventionally, friction force (F_f) between two surfaces is proportional to the applied normal force (F_N). This linear relation between F_f and F_N is explained by the well-known Amontons' law, which states that the real contact area (A_{real}) between two macroscale surfaces is generally proportional to F_N[3,4]; thus, if the shear stress on A_{real} is reasonably assumed to be constant, then the linear relations $F_f \propto A_{real} \propto F_N$ appear. Recently, however, with the advances in nanotribological experiments, it has been found that frictional behavior at nanoscale contact does not generally obey Amontons' law[5,6]. Instead, nanoscale friction behaves like a thermally activated process[7], and various analytical models have been established to explain the nanoscale friction data. For example, by treating nanoscale friction as a point-contact scheme in which a contacting atom is thermally activated to scan over a corrugated potential surface, successful predictions have been made regarding how the friction force of this contacting atom varies with temperature and scanning velocity, such as the Prandtl–Tomlinson (PT) model and its extended theories[8–11]. Moreover, recent works have shown that nanoscale frictional behavior is dominated by the thermally activated formation of interfacial chemical bonds[12], and thus the corresponding F_f at nanoscale contact is proportional to the number of atoms that have interfacial chemical bonds[13–15]. Based on the scheme in which interfacial chemical bonds are formed and ruptured repeatedly

during the friction, a recently proposed multi-bond analytical model of nanoscale friction offered a good interpretation of experimental data under various external conditions[5,16–19].

However, even though the aforementioned works are unquestionably useful in understanding nanoscale friction partially, experimental insights into the thermally activated friction processes are far below what is needed in practice. To predict practically the atomic-scale friction, the crucial first step is to obtain the exact number of atoms having interfacial chemical bonds (N_{ib}) and the mean shear force per interfacial bond (F_{ib}), according to the detailed external conditions (applied normal force, sliding velocity, and environmental temperature), material properties (e.g., Young's modulus and density), and surface morphology (determining the real contact area). Because both the forming and rupturing of interfacial bonds are chemical reactions, N_{ib} and F_{ib} can be calculated via the reaction rate theory by introducing several semi-empirical parameters such as the activation energy of interfacial bond formation, just like what the PT and multi-bond models have done. Once these semi-empirical parameters, material properties, and surface morphology are known, it is possible to predict how the external conditions affect the friction force at the atomic scale. Generally, exact values of these semi-empirical parameters should be extracted from experimental results of N_{ib} and F_{ib} at different surface temperatures as actually experienced by atoms in the real contact surface, because both the forming and rupturing of interfacial bonds are temperature-dependent processes. However, for experiments, N_{ib}, F_{ib}, and the real surface temperature are extremely difficult to be precisely measured even using the most advanced experimental instruments, although it is easy to experimentally obtain other required information such as applied loads, sliding velocities, Young's modulus, and surface roughness. This lack of correct values for N_{ib}, F_{ib}, and the real surface temperature directly hinders the development and validation of a practically applicable friction law. In this paper, we propose that the interfacial

chemical reactions and real surface temperature could be monitored very effectively and precisely using the large-scale reactive molecular dynamics (MD) simulations with our previously developed high-accuracy reactive potentials[20–22]. We aim to establish a practically and easily applicable friction law that can predict how the friction force varies with the external conditions at the atomic scale, based on the precisely measured N_{ib}, F_{ib}, and surface temperature from MD simulations.

Results

We use diamond-like carbon (DLC)[23,24] as the test material because DLC is a widely used and studied solid lubricant. Fig. 1A shows the friction simulation model, in which two hydrogen-passivated DLC substrates with self-affine roughness[25] are used to represent a realistic contact state. The rigid layer of the upper substrate is loaded with a normal force (F_N) and slid forcibly with a sliding velocity (v), while the rigid layer of the lower substrate is kept stationary. Temperature of the thermostat layers neighboring the rigid layers, which is regarded as the substrate temperature (T_{sub}), is controlled during the friction simulation. Obviously, the real temperature of contacting surface (T_{real}) is higher than T_{sub} because of the frictional heat at the friction interface. Therefore, to obtain the exact T_{real} and then understand how it influences the friction force and interfacial chemical reactions, we perform friction simulations with different T_{sub} while keeping F_N and v unchanged. To obtain the accurate T_{real} in MD, temperature distributions in the substrate depth direction are investigated, as exemplified in Fig. 1B where T_{sub} = 300 K, F_N = 675 nN, and v = 100 m/s. Initially, temperature of the whole substrate is distributed homogeneously and is around 300 K; however, during friction, temperature increases with proximity to the friction interface. Here, T_{real} is defined as the mean of the highest

temperature in the distribution profile, which is about 500 K higher than T_{sub}. Using this definition, we observe that the obtained T_{real} increases almost linearly with increasing T_{sub} (Fig. 1C). See the Supplementary Information for detailed simulation setups and discussions on T_{real}.

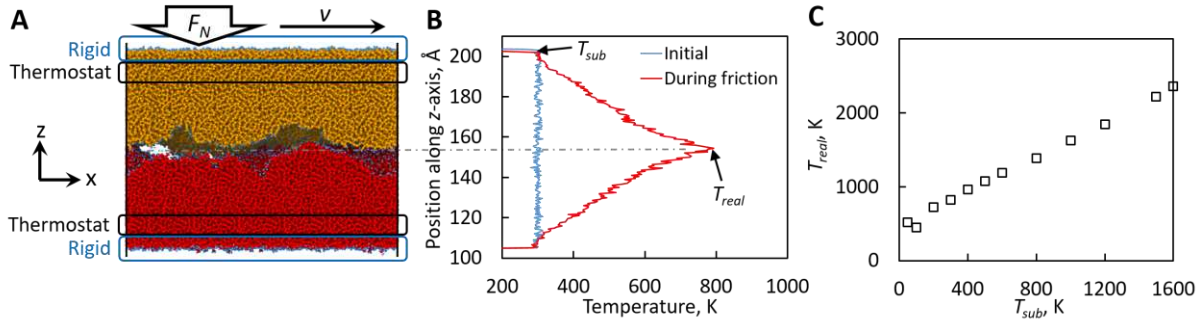

Fig. 1 Simulation setup and calculation of T_{real}. (A) Simulation model of two rough surfaces. Blue balls represent hydrogen atoms, while orange and red ones represent carbon atoms in the upper and lower substrate, respectively. (B) Temperature distribution of a typical friction simulation with T_{sub} = 300 K, F_N = 675 nN, and v = 100 m/s. (C) T_{real} as a function of T_{sub} under the same F_N and v as in (B).

The next task is to know how friction force (F_f) and interfacial chemical reactions are affected by T_{real} in the MD simulations. Open squares in Fig. 2A show the MD-measured F_f as a function of T_{real}, where an interesting mountain-type temperature dependence of F_f appears. What is the origin of this F_f-T_{real} relationship? At atomic scale, F_f is essentially proportional to the total number of atoms having interfacial chemical bonds (N_{ib})[13–15]; thus, if F_{ib} represents the mean shear force per interfacial bond, F_f can be calculated by

$$F_f = \frac{N_{ib}F_{ib}}{2} \quad (1)$$

where the product of N_{ib} and F_{ib} is halved because the upper and lower substrates are assumed to contain the same number of interfacial bonding atoms. Thus, we can now study how T_{real} affects N_{ib} and F_{ib} separately. Figs. 2B and 2C show the results of N_{ib} and F_{ib} respectively as a function of T_{real} which are directly measured from the MD simulations. Qualitatively, N_{ib} increases whereas F_{ib} deceases non-linearly with the increasing T_{real}, and hence the competition of the increasing N_{ib} and decreasing F_{ib} is suggested to be the origin of the mountain-type F_f-T_{real} relationship.

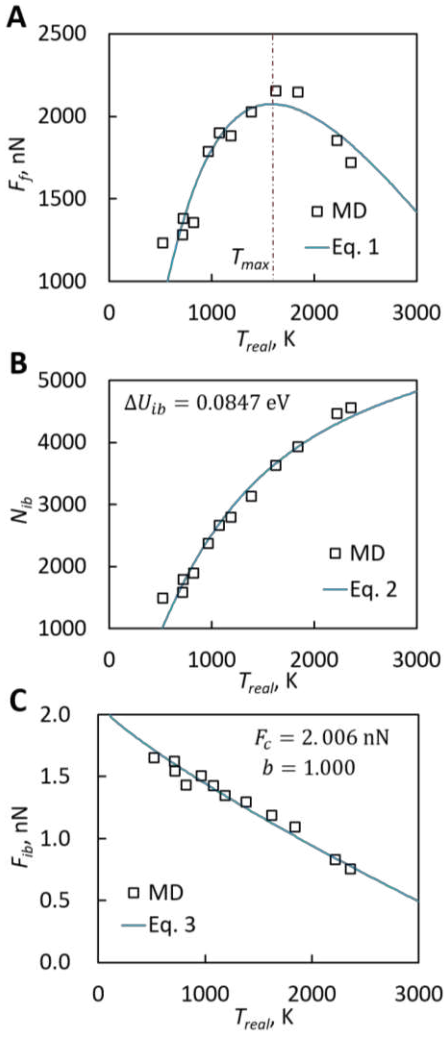

Fig. 2 Friction simulation results. (A) N_{ib}, (B) F_{ib}, and (C) F_f as a function of T_{real} with F_N = 675 nN and v = 100 m/s.

Next, we discuss quantitatively how T_{real} influences N_{ib} and F_{ib}. For N_{ib}, because only the atoms in the real contact area have opportunities to form chemical bonds with their counterparts, N_{ib} can be computed by multiplying the number of atoms in the real contact region ($2A_{real}(F_N)/A_{atom}$, where the real contact area $A_{real}(F_N)$ is a function of F_N and A_{atom} is the average surface area per atom) with the probability of forming an interfacial bond. As we have reported previously[26], this probability is affected by both temperature (T) and applied normal force (F_N), and can be computed by applying the reaction rate theory[27,28] to the reaction of interfacial bond formation. Thus, the expression of N_{ib} as a function of T and F_N is

$$N_{ib}(T, F_N) = \frac{2A_{real}(F_N)}{A_{atom}} \exp\left[\frac{V_{atom}}{2Ek_BT}\left(\frac{F_N}{A_{real}(F_N)}\right)^2 - \frac{\Delta U_{ib}}{k_BT}\right] \quad (2)$$

where V_{atom} is the average volume per atom, E is the Young's modulus, k_B is the Boltzmann constant, and ΔU_{ib} is the activation energy of forming an interfacial bond. $A_{real}(F_N)$, A_{atom}, V_{atom}, and E can be obtained directly if the material properties and surface morphology are known, but ΔU_{ib} still needs to be determined from experimental and/or simulation fitting (see the Supplementary Information for detailed discussion). In Fig. 2B, Eq. 2 reproduces the MD results of N_{ib} very well if ΔU_{ib} = 0.0847 eV and $T = T_{real}$ are used. Here it should be additionally but interestingly noticed that Eq. 2 with $T = T_{sub}$ could not fit the MD results whatever (Fig. S3 in the Supplementary Information), indicating that the one which truly dominates the thermally activated friction process is T_{real} rather than T_{sub} or the environmental temperature. Meanwhile, the lateral force of rupturing an interfacial bond, F_{ib}, could be correctly obtained by the multi-bond model

proposed by Urbakh's group[5,16–19]. However, Urbakh's multi-bond model is too complex to be applied simply, because its analytical expression involves multiple hard-to-determine empirical parameters. Instead, F_{ib} can be estimated by the simpler PT model because the thermally activated process of rupturing an interfacial bond can be regarded as the process of climbing a potential curve. Using a previous form[9], we have

$$F_{ib}(T, v) = F_c - \left[\beta k_B \ln\left(\frac{bT}{v}\right)\right]^{\frac{2}{3}} T^{\frac{2}{3}} \quad (3)$$

where β is potential curve corrugation of contact surface and is a function of the critical force (F_c). b is a material- and system-dependent parameter as discussed exhaustively in the Supplementary Information. Here, only F_c and b as fitting parameters should be determined by comparing with the experimental/simulation results. By fitting Eq. 3 to the MD-measured F_{ib} using $T = T_{real}$, we obtain F_c = 2.006 nN and b = 1.000. Thus, with the values obtained above for ΔU_{ib}, F_c, and b, Eq. 1 succeeds to predict a mountain-type temperature dependence of the friction force, which matches the MD-measured F_f perfectly (Fig. 2A).

It is also essential to precisely understand the frictional behaviors as well as the interfacial chemical reactions affected by different F_N and v, and we expect Eqs. 1–3 (with the above extracted ΔU_{ib}, F_c, and b) to be valid for describing the load and velocity effects. According to Eqs. 2 and 3, it is obvious that, if temperature is unchanged, F_N and v would only have influences on N_{ib} and F_{ib}, respectively. Thus, to check the relationship between N_{ib} and F_N and assess the validity of Eq. 2, we perform friction simulations using the same model as that in Fig. 1A, by varying F_N while keeping T_{sub} = 300 K and v = 100 m/s; thereafter, to study the $F_{ib}(v)$, simulations are performed by varying v while keeping T_{sub} = 300 K and F_N = 675 nN. Open squares in Figs. 3A and 3B show the simulation results of N_{ib} and F_{ib} as a function of F_N and v,

respectively. Focusing on $N_{ib}(F_N)$ firstly, the measured N_{ib} increases monotonically with F_N, and then we should confirm whether this relationship obeys Eq. 2 or not. Note that T_{real} will increase with F_N even though T_{sub} is kept unchanged because larger applied load brings more frictional heat (Fig. S2A in the Supplementary Information). Obviously, to predict $N_{ib}(F_N)$, the exact values of T_{real} must be taken into consideration; otherwise, for instance, if $T = T_{sub}$ is substituted into Eq. 2, the prediction (red line in Fig. 3A) differs greatly from the simulation results. However, if $T = T_{real}$ (which is obtained with respect to each F_N) is used, the prediction agrees with the simulation results very well (blue line in Fig. 3A). Meanwhile, for $F_{ib}(v)$, the MD simulations show a decreasing trend of F_{ib} with increasing v. As with the load-induced change of T_{real}, increasing v also cause a raise of T_{real} because of the higher frictional heat (Fig. S2B in the Supplementary Information). Therefore, to correctly predict $F_{ib}(v)$, we must use the exact values of T_{real}; otherwise, for instance, the predicted F_{ib} using $T = T_{sub}$ exhibits a positive correlation with v (red line in Fig. 3B), which differs completely from the simulation results. However, if $T = T_{real}$ (which is obtained with respect to each v) is substituted to Eq. 3, the predictions show an agreement with the MD simulation results (blue line in Fig. 3B). Overall, the above results demonstrate that Eqs. 1–3 are indeed valid for describing nanoscale friction behavior under different applied loads and sliding velocities, but only if using the correct surface temperature rather than the substrate or environmental temperature.

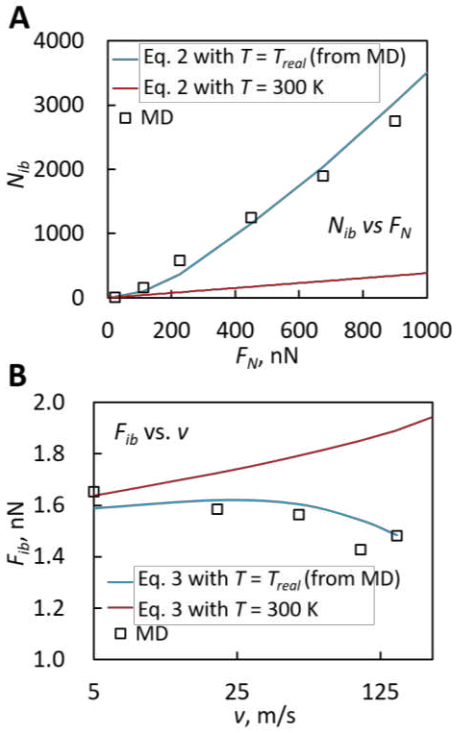

Fig. 3 Validation of load and velocity effects. (A) N_{ib} as a function of F_N with T_{sub} = 300 K and v = 100 m/s. (B) F_{ib} as a function of v with T_{sub} = 300 K and F_N = 675 nN; note the use of a logarithmic coordinate for v (abscissa).

Here, as a trial application of Eqs. 1–3, we predict how F_N and v affect the temperature dependence of F_f. In Fig. 2C, F_f exhibits a mountain-like dependence on T_{real} under constant F_N and v. According to Eqs. 2 and 3, this temperature dependence of friction may be altered by F_N and v through their effects on N_{ib} and F_{ib}, respectively. Fig. 4A shows the predicted F_f as a function of T_{real} under a constant v of 100 m/s but different F_N. With increasing F_N, the F_f-T_{real} curve moves upward entirely because of the increasing N_{ib} with F_N, while the critical temperature corresponding to the maximum friction (referred as to T_{max}) remains unchanged. Regarding the velocity effect, Fig. 4B shows the predicted F_f under a constant F_N of 675 nN but different v.

Herein we observe the entire shift-up of the curve with the increasing v again, but interestingly the T_{max} increases with increasing v, differing from the load effect. The above predicted trends, namely, that the sliding velocity changes T_{max} whereas the applied load does not, agree qualitatively with previous experiments[19,29]. This result helps the reduction of friction by choosing the proper temperature and sliding velocity, thereby benefiting greatly the practical design of lubricating systems.

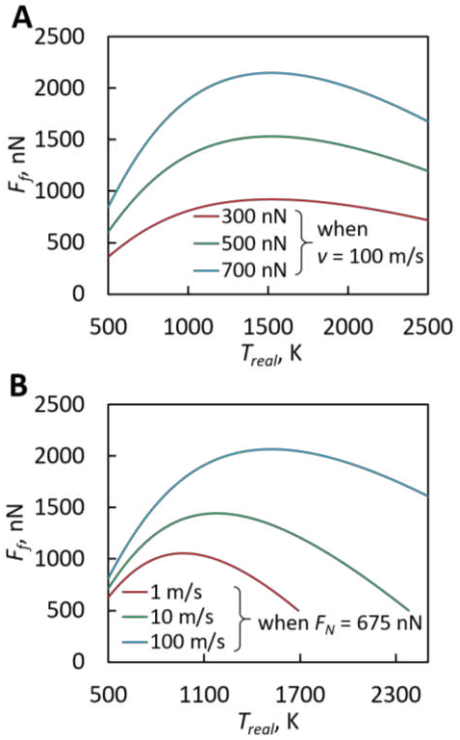

Fig. 4 Effects of F_N and v on temperature dependence of F_f. (A) F_f as a function of T_{real} under a constant v of 100 m/s but different F_N. (B) F_f as a function of T_{real} under a constant F_N of 675 nN but different v.

We must also point out the limitations of Eqs. 1–3 for friction prediction. First, they are not available for the systems in which non-bonding interactions such as van der Waals are dominant.

Such systems include (i) atomic-scale contact of ultra-smooth surfaces (because surface adhesion becomes a dominant factor with decreasing surface roughness[30,31]) and (ii) friction of two-dimensional materials such as graphene and MoS_2 (because friction of these materials stems mostly from the van der Waals interactions between neighboring layers). Second, Eqs. 1–3 may fail under extremely high or low temperatures, loads, and sliding velocities, as discussed exhaustively in the Supplementary Information.

Discussion

In summary, we succeeded in using large-scale reactive MD simulations to precisely monitor the real surface temperature and interfacial chemical reactions of DLC in a realistic rough-surface contact state. Based on the MD simulation results, we established a proper theoretical friction law to describe the atomic-scale frictional behavior and further predict how the friction force varies with temperature, sliding velocity, and applied load. Furthermore, we showed that the actual temperature of the contacting surface must be used in the proposed friction model to practically and correctly predict the friction force; otherwise, the predictive results may deviate greatly if the substrate or environmental temperature is used in the proposed friction law. This work could contribute greatly to understanding the fundamentals of friction and the practical design of lubricating systems.

References

1. Szeri, A. Z. *Tribology: friction, lubrication, and wear*. (Hemisphere Pub. Corp., 1980).
2. Holmberg, K. & Erdemir, A. Global impact of friction on energy consumption, economy and environment. *FME Trans.* **43**, 181–185 (2015).

3. Greenwood, J. A. & Williamson, J. B. P. Contact of nominally flat surfaces. *Proc. R. Soc. A Math. Phys. Eng. Sci.* **295**, 300–319 (1966).

4. Persson, B. N. J. Theory of rubber friction and contact mechanics. *J. Chem. Phys.* **115**, 3840–3861 (2001).

5. Ouyang, W. *et al.* Load and velocity dependence of friction mediated by dynamics of interfacial contacts. *Phys. Rev. Lett.* **123**, 116102 (2019).

6. Weber, B. *et al.* Molecular probes reveal deviations from Amontons' law in multi-asperity frictional contacts. *Nat. Commun.* **9**, 888 (2018).

7. Spikes, H. Stress-augmented thermal activation: Tribology feels the force. *Friction* **6**, 1–31 (2018).

8. Jansen, L., Hölscher, H., Fuchs, H. & Schirmeisen, A. Temperature dependence of atomic-scale stick-slip friction. *Phys. Rev. Lett.* **104**, 256101 (2010).

9. Riedo, E., Gnecco, E., Bennewitz, R., Meyer, E. & Brune, H. Interaction Potential and Hopping Dynamics Governing Sliding Friction. *Phys. Rev. Lett.* **91**, 084502 (2003).

10. Liu, X. Z. *et al.* Dynamics of atomic stick-slip friction examined with atomic force microscopy and atomistic simulations at overlapping speeds. *Phys. Rev. Lett.* **114**, 146102 (2015).

11. Sang, Y., Dubé, M. & Grant, M. Thermal effects on atomic friction. *Phys. Rev. Lett.* **87**, 174301 (2001).

12. Wang, Y. *et al.* Tribochemical reactions and graphitization of diamond-like carbon against alumina give volcano-type temperature dependence of friction coefficients: A tight-binding quantum chemical molecular dynamics simulation. *Carbon* **133**, 350–357 (2018).

13. Mo, Y., Turner, K. T. & Szlufarska, I. Friction laws at the nanoscale. *Nature* **457**, 1116–1119 (2009).

14. Mo, Y. & Szlufarska, I. Roughness picture of friction in dry nanoscale contacts. *Phys. Rev. B* **81**, 035405 (2010).

15. Li, Q., Tullis, T. E., Goldsby, D. & Carpick, R. W. Frictional ageing from interfacial bonding and the origins of rate and state friction. *Nature* **480**, 233–236 (2011).

16. Dudko, O. K., Filippov, A. E., Klafter, J. & Urbakh, M. Beyond the conventional description of dynamic force spectroscopy of adhesion bonds. *Proc. Natl. Acad. Sci.* **100**, 11378–11381 (2003).

17. Filippov, A. E., Klafter, J. & Urbakh, M. Friction through dynamical formation and rupture of molecular bonds. *Phys. Rev. Lett.* **92**, 2–5 (2004).

18. Barel, I., Urbakh, M., Jansen, L. & Schirmeisen, A. Multibond dynamics of nanoscale friction: The role of temperature. *Phys. Rev. Lett.* **104**, 066104 (2010).

19. Barel, I., Urbakh, M., Jansen, L. & Schirmeisen, A. Unexpected temperature and velocity dependencies of atomic-scale stick-slip friction. *Phys. Rev. B* **84**, 115417 (2011).

20. Wang, Y. *et al.* Triboemission of hydrocarbon molecules from diamond-like carbon friction interface induces atomic-scale wear. *Sci. Adv.* **5**, eaax9301 (2019).

21. Wang, Y. *et al.* Reactive molecular dynamics simulations of wear and tribochemical reactions of diamond like carbon interfaces with nanoscale asperities under H_2 gas: Implications for solid lubricant coatings. *ACS Appl. Nano Mater.* **3**, 7297–7304 (2020).

22. Wang, Y. *et al.* Proposal of a new formation mechanism for hydrogenated diamond-like carbon transfer films: hydrocarbon-emission-induced transfer. *Carbon* **154**, 7–12 (2019).

23. Erdemir, A. & Donnet, C. Tribology of diamond-like carbon films: recent progress and future prospects. *J. Phys. D. Appl. Phys.* **39**, 311–327 (2006).

24. Al Mahmud, K. A. H., Kalam, M. A., Masjuki, H. H., Mobarak, H. M. & Zulkifli, N. W. M. An updated overview of diamond-like carbon coating in tribology. *Crit. Rev. Solid State Mater. Sci.* **40**, 90–118 (2014).

25. Yan, W. & Komvopoulos, K. Contact analysis of elastic-plastic fractal surfaces. *J. Appl. Phys.* **84**, 3617–3624 (1998).

26. Wang, Y. *et al.* Non-empirical law for nanoscale atom-by-atom wear. *Adv. Sci.* **7**, 2002827 (2020).

27. Hänggi, P., Talkner, P. & Borkovec, M. Reaction-rate theory: fifty years after Kramers. *Rev. Mod. Phys.* **62**, 251–341 (1990).

28. Jacobs, T. D. B., Gotsmann, B., Lantz, M. A. & Carpick, R. W. On the application of transition state theory to atomic-scale wear. *Tribol. Lett.* **39**, 257–271 (2010).

29. Barel, I., Urbakh, M., Jansen, L. & Schirmeisen, A. Temperature dependence of friction at the nanoscale: When the unexpected turns normal. *Tribol. Lett.* **39**, 311–319 (2010).

30. Jacobs, T. D. B. *et al.* The effect of atomic-scale roughness on the adhesion of nanoscale asperities: A combined simulation and experimental investigation. *Tribol. Lett.* **50**, 81–93 (2013).

31. Ryan, K. E. *et al.* Simulated adhesion between realistic hydrocarbon materials: Effects of composition, roughness, and contact point. *Langmuir* **30**, 2028–2037 (2014).

Data availability

All data needed to evaluate the conclusions are present in the paper and/or the Supplementary Information. Additional data are available from the authors upon request.

Acknowledgments

This research was supported by MEXT as "Exploratory Challenge on Post-K Computer" (Challenge of Basic Science - Exploring Extremes through Multi-Physics and Multi-Scale Simulations), JST CREST, JSPS Grant-in-Aid for Young Scientists (B) (Grant No. 17K14430), JSPS Grant-in-Aid for Scientific Research (C) (Grant No. 19K05380), and JSPS Grant-in-Aid for Scientific Research (A) (Grant No. 18H03751). We gratefully acknowledge the Center for Computational Materials Science (CCMS, Tohoku University) for the use of MAterials science Supercomputing system for Advanced MUlti-scale simulations towards NExt-generation - Institute for Materials Research (MASAMUNE-IMR) (Grant Nos. 18S0403 and 19S0506).

Author contributions

M.K. supervised the research. Y.W. conceived the main idea of this work, and then designed and performed the simulations. J.X. prepared the simulation code framework. The manuscript was written by Y.W. and revised by J.X., K.A., and M.K. All authors participated in the interpretation of the data and discussion of the manuscript.

Competing interests

The authors declare no competing interests.

Figures

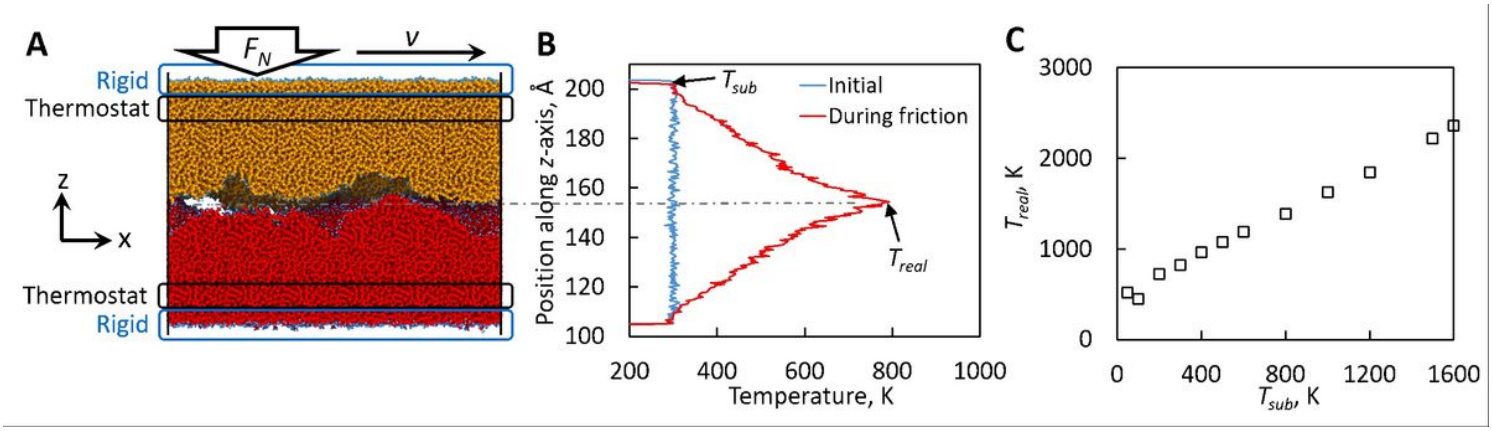

Figure 1

Simulation setup and calculation of Treal. (A) Simulation model of two rough surfaces. Blue balls represent hydrogen atoms, while orange and red ones represent carbon atoms in the upper and lower substrate, respectively. (B) Temperature distribution of a typical friction simulation with Tsub = 300 K, Fn = 675 nN, and = 100 m/s. (C) Treal as a function of under the same Fn and v as in (B).

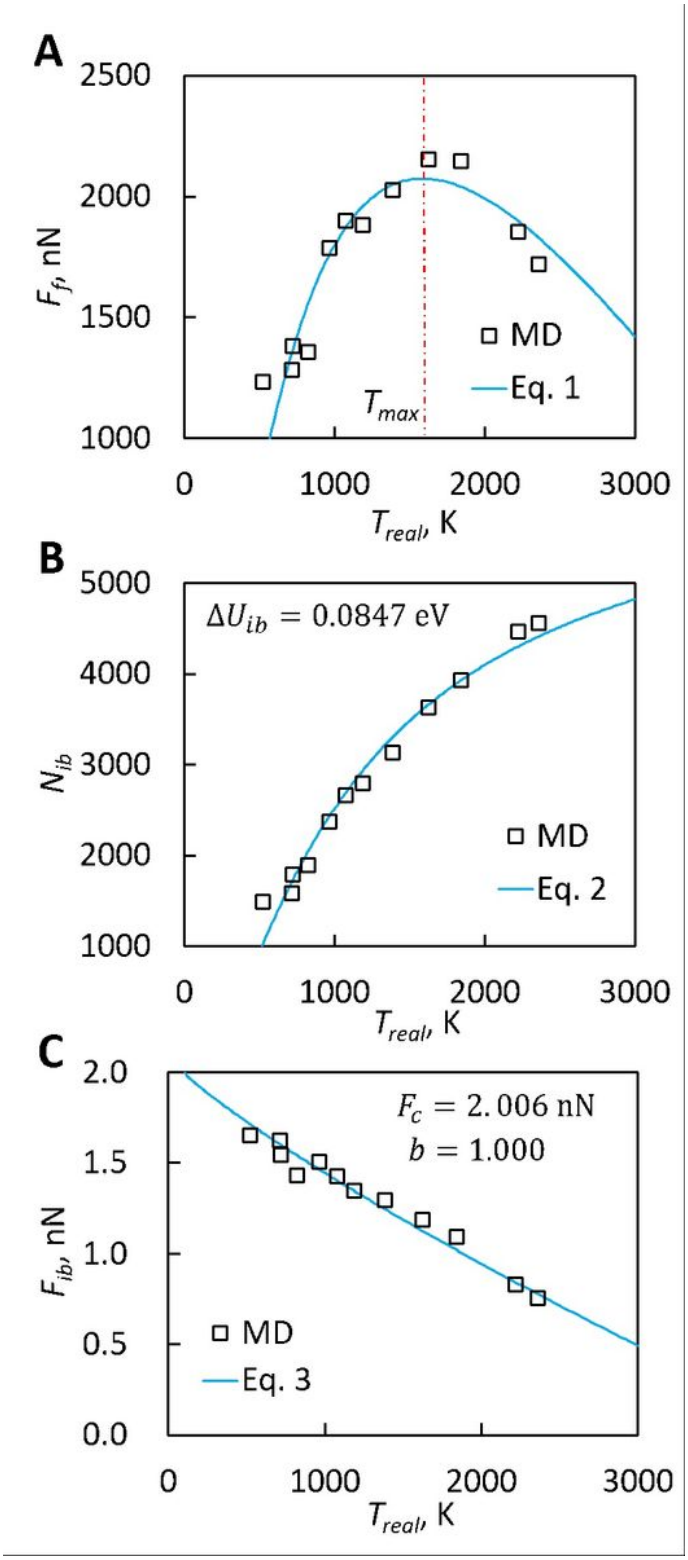

Figure 2

Friction simulation results. (A) Nib , (B) Fib , and (C) Ff as a function of Treal with Fn = 675 nN and v = 100 m/s. s.

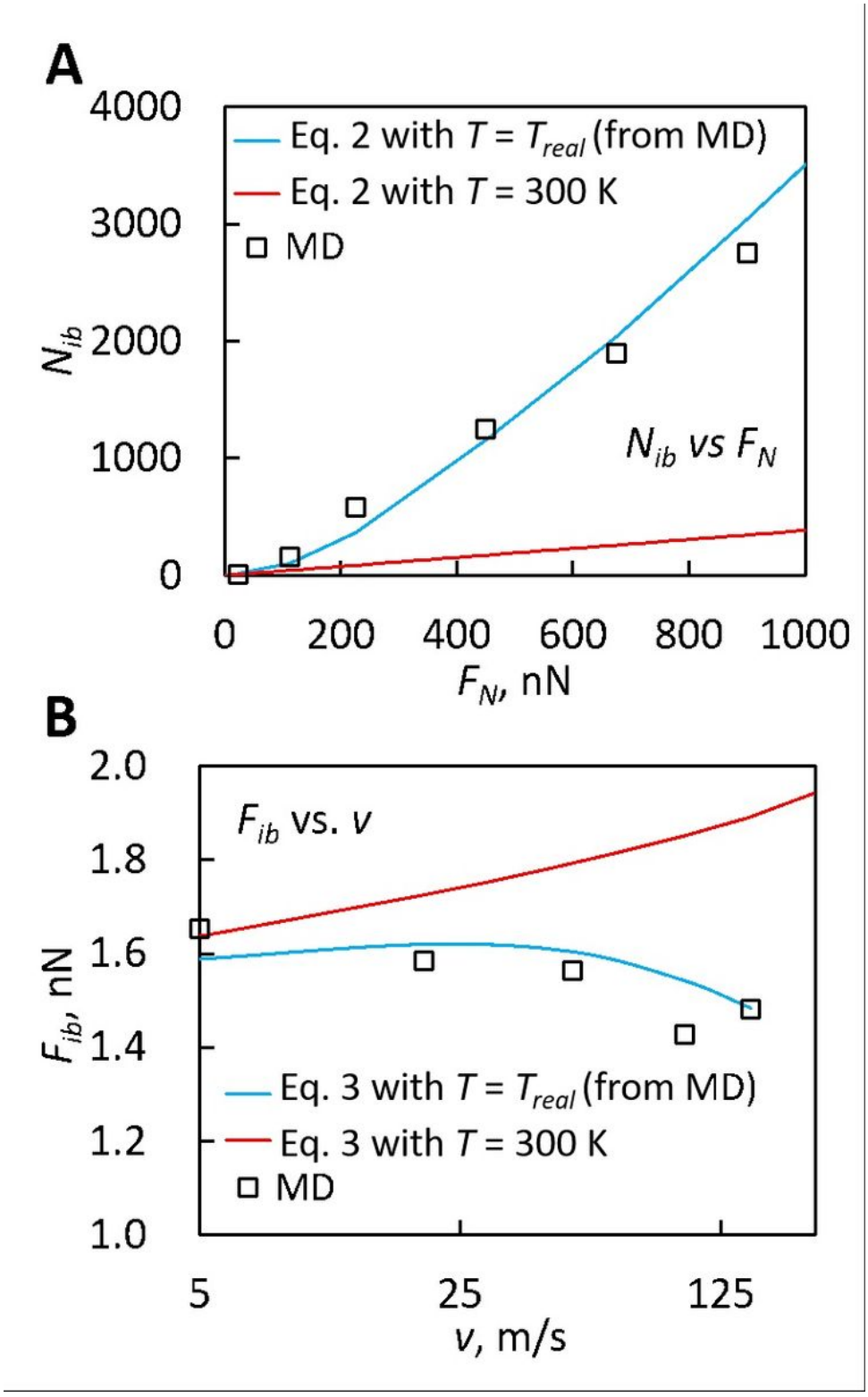

Figure 3

Validation of load and velocity effects. (A) Nib as a function of Fn with Tsub = 300 K and v = 100 m/s. (B) as a function of v with Tsub = 300 K and Fn = 675 nN; note the use of a logarithmic coordinate for v (abscissa).

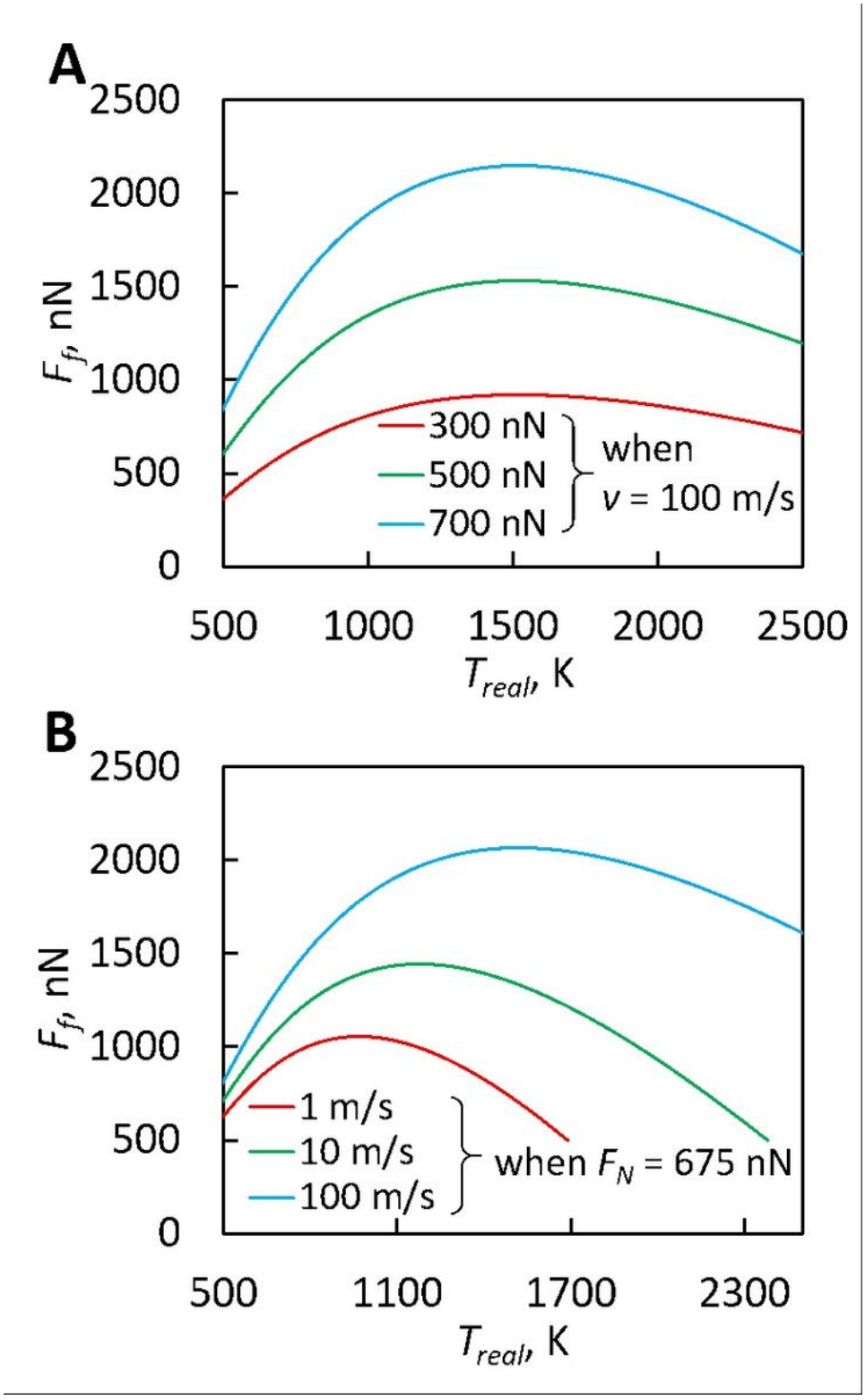

Figure 4

Effects of Fn and v on temperature dependence of Ff. (A) as a function of Treal under a constant v of 100 m/s but different . (B) as a function of Treal under a constant Fn of 675 nN but different v.

Supplementary Files

This is a list of supplementary files associated with this preprint. Click to download.

- Supplementary.docx